

Spatial Disorder and Degradation Kinetics in Intrinsic Biodegradation Schemes

Randall A. LaViolette,^{*,†} M. E. Watwood,[‡] T. R. Ginn,[§] and D. L. Stoner[†]

Idaho National Engineering and Environmental Laboratory, P.O. Box 1625, Idaho Falls, Idaho, 83415-2208, Department of Biological Sciences, Idaho State University, Pocatello, Idaho, 83209-8007, and Department of Civil and Environmental Engineering, University of California - Davis, Davis, California 95616

Received: December 7, 1998; In Final Form: April 7, 1999

The restoration of contaminated soils by intrinsic biodegradation employs microorganisms in the subsurface that degrade the contaminant substrate infiltrating the subsurface matrix. The outcome of intrinsic biodegradation has been difficult to predict. We examine a source of the difficulty with a computational model of diffusive-reactive transport that introduces spatial disorder in the arrangement of the degrading microorganisms. Spatial disorder alone, even on the small scales that characterize the distance between aggregates of microorganisms, is enough to induce a wide range of times to complete the degradation to an arbitrary limit. The mean time for the concentration to achieve the limit becomes twice that for the case of spatial order. Bounds on the range of the effective degradation kinetics can be obtained by computing the distribution of times to complete degradation.

I. Introduction

Intrinsic biodegradation has gained widespread attention as a remedial option at many sites.¹ Biodegradation takes advantage of the subsurface microbial communities that degrade organic contaminants.^{2–4} Intrinsic biodegradation is considered feasible as a restoration technique when indigenous subsurface microbial communities transform the contaminants to an acceptable concentration and within an acceptable time interval.¹ Therefore we are concerned in this work with the question: “How long will intrinsic biodegradation take?” It turns out that biodegradation in the field often requires more time than what would have been predicted from the degradation rates measured in the laboratory.^{5–7} There are myriad plausible explanations for this type of discrepancy, including competition for nutrients and other trophic interactions, toxicity responses, and threshold effects.⁵ Each of these explanations depends on the circumstances at a particular contaminated site, and each explanation requires characterization studies that might never be carried out. Instead, we will show how the disorder in the placement of microorganisms in an otherwise homogeneous subsurface can contribute to this discrepancy.

Here we are concerned with the consequences of disorder in the trap locations upon the large-scale degradation kinetics of a fluid contaminant substrate in a homogeneous matrix. Our motivation comes from the theoretical demonstration that spatial fluctuations in the distances between randomly located traps can introduce kinetic or transport anomalies in a variety of circumstances.^{8,9} The picture that emerges from those studies is that in an ordered or homogeneous system, all locations are equally “dangerous” for the diffusing substrate; in the disordered system, trap-free regions appear where the substrate can remain “safe” for long times. The theoretical results suggested to us that investigation of similar behavior for a model intrinsic biodegradation process would be worthwhile. The plausible

assumption that spatial fluctuations in trap positions, because they occur on relatively small distance scales, would not qualitatively affect macroscale transport is routinely invoked to reduce the effort involved in transport calculations. In most transport calculations, spatial averages are performed over distances far in excess of those that describe the fluctuations in trap positions, thereby averaging away *a priori* the fluctuations that might result from random trapping. Although many plausible justifications can be invoked for this kind of averaging, this crucial assumption deserves a direct test. Such a test is the goal of this paper.

II. Diffusion-Reaction Model

We seek to understand the discrepancy in degradation rates between laboratory studies and field observations with a computational study of a simple mathematical model. Our assumptions for the kind of system under investigation here include (i) degradation occurs at a finite number of traps randomly distributed in the subsurface;^{10,11} (ii) traps are localized colonies of microorganisms that do not move, grow, or die but irreversibly remove (i.e., immobilize or transform) contaminant substrate at a finite rate, described by the Michaelis–Menten rate law;⁵ (iii) the subsurface matrix itself is sufficiently homogeneous to exclude transport anomalies arising in the absence of traps (anomalies arising purely from heterogeneities in the matrix are elucidated in ref 12); (iv) transport is essentially diffusive.

As indicated in assumption (iv) above, the scope of this study is restricted to diffusive transport regimes, reflecting low Peclet number ($Pe < 1$) transport by groundwater. This case provides a simplified starting point for study of the effect of biochemical heterogeneity on field-scale solute degradation and is also a reasonable representation of fate and transport processes at sites involving low or no convection. Examples include contamination of deep regional aquifers in semiarid environments, near-surface contamination of soils with low hydraulic conductivity, and other contaminated groundwater environments targeted restoration by intrinsic biodegradation strategies that are absent of flow

* To whom correspondence should be addressed (e-mail: yaq@inel.gov).

† Idaho National Engineering and Environmental Laboratory.

‡ Idaho State University.

§ University of California.

acceleration measures.¹³ The incorporation of convective and dispersive processes would have a limiting effect on the residence time of the substrate (with respect to the fixed traps) and therefore would affect the outcome of intrinsic biodegradation, but this is beyond the scope of our work. A system dominated by convection would be much less prone to the anomalies we report below; however, such a system would not be considered for bioremediation in the first place, because of the short residence time near each trap that such convection would impose. Thus we dropped the advection term in the transport equation that is usually employed to describe subsurface contaminant transport.¹⁴

Next, we consider the transport, then the degradation kinetics, of the substrate and combine the two into a simple model below. The kinetics of many of the most useful biodegradation processes (in which the microorganisms consume substrate but do not grow) are often well-described by the venerable Michaelis–Menten (or “Monod-no-growth”) rate law,⁵ which is nonlinear in the concentration, as follows:

$$\frac{dc(t)}{dt} = \frac{-Rc(t)}{c^+ + c(t)} \quad (1)$$

where c is the volumetric mass concentration of the substrate, $R > 0$ is the volumetric mass removal rate, $c^+ < c(0)$ is a concentration “half-saturation”, and t is time. The Michaelis–Menten rate law is an empirical interpolation between two observed regimes of degradation behavior. For $c \gg c^+$, the degradation rate nearly follows zeroth-order kinetics (rate is independent of concentration), so that c declines linearly with time. For $c \ll c^+$, the degradation rate nearly follows first-order kinetics (rate is linear in concentration), so that c decays exponentially with time. The most effective of these two regimes for biodegradation should be the zeroth-order regime.¹⁵ However, the zeroth-order rate law by itself would give overly optimistic predictions regarding the time required to reach a particular endpoint concentration. The first-order regime with its essentially exponential decay tends to lengthen the time required for a degradative process to achieve a specified contaminant concentration. The time t^* when the contaminant concentration “crosses over” from essentially zeroth-order to first-order rate law can be used to define the most significant interval for a given degradative process (alternatively, the “half-life” $t_{1/2}$ is also often reported;¹⁶ here, $t_{1/2} \approx t^*/2$). This type of crossover has been observed for the biodegradation of several organic chemicals, including maleic hydrazide in soil and glucose and linear alcohols in bay water.⁵ The crossover time may correspond to the inflection point on a typical “diminishing returns curve” that relates the desired endpoint concentration to the cost that is required to achieve the endpoint. This type of plot is often generated during negotiations with regulatory officials in order to establish remediation endpoint concentrations, in cases where such endpoints are otherwise unclear.¹⁷

Our model combines the reaction kinetics and the diffusive transport of the substrate. We represent the subsurface matrix as an evenly spaced linear lattice of N nodes; thus the matrix would be homogeneous apart from the traps. In a two- or three-dimensional flow, this lattice would be best taken to correspond to a transverse direction of a constant-velocity flow, in keeping with our intent to model essentially diffusive transport. The distance between nodes Δx is set to λ/n , where λ is the mean distance between traps and n is chosen so that there are on average $(n - 1)$ nodes between each trap. The relation between

the time t , position x , and degradation rate R to their dimensionless counterparts τ , ν , and ρ is given by

$$\begin{aligned} x &\equiv \nu \frac{\lambda}{n} \\ t &\equiv \tau \frac{(\lambda/n)^2}{D} \\ \rho &\equiv \frac{\lambda^2 R}{n^2 D} \end{aligned} \quad (2)$$

respectively where ν is an integer that labels the nodes. In these dimensionless units, which we employ hereafter, the distance between nodes (Δx) is unity, as is the diffusion constant D , and the relationship between the mass transport and the degradation rate is absorbed in the specification of ρ . Combining all of these considerations produced the desired diffusion-reaction equation for the substrate:

$$\frac{dc_\nu(\tau)}{d\tau} = \frac{c_{\nu+1}(\tau) + c_{\nu-1}(\tau) - 2c_\nu(\tau)}{\nabla^2 c} - \frac{\rho_\nu c_\nu(\tau)}{c_\nu^+ + c_\nu(\tau)} \quad (3)$$

The first term on the right-hand side of (3) represents diffusion on the lattice. The second term on the right-hand side of (3) is the discretized degradation rate. The effect of the discretization on this term is to limit the range of the interaction of the trap to the space halfway between each of the neighboring nodes.

Next, we considered two cases for the trap distributions:

P (periodic)

$$\begin{aligned} \rho_\nu &= \gamma \text{ (a positive constant) if } \nu \text{ is a multiple of } n, \\ &= 0 \text{ otherwise} \end{aligned}$$

R (random) $\rho_\nu = \gamma$ with probability $1/n$, $\rho_\nu = 0$ otherwise

In each case the traps remain fixed on the lattice. Case P corresponds to the common practice, where the mean degradation rate parameter taken from the laboratory is inserted into a model for transport of the fluid in the matrix. The periodic distribution implements the mean degradation rate assumption for this model. Case R corresponds to the situation where each configuration has a disordered placement of traps arising out of the same “uniform random” distribution, but each configuration has a different placement of traps from any other configuration. The distribution of traps in case R is not quite uniformly random, because we require that no two traps can be closer to each other than the lattice spacing λ/n . In this work the degradation rate is the same for each trap, although it would have been easy to impose a distribution of trap rates as well as trap locations.

To solve (3), we need to specify n , the initial conditions, the boundary conditions, c^+ , and γ for the cases P and R, respectively. We set $n = 10$ throughout. We imposed the Dirichlet condition for the endpoints ($c_N = c_{-N} = 0$) and adjusted N so that the concentration near either of the boundaries was always negligible ($2500 \leq N \leq 5000$). The initial unit mass (or volume) of the substrate ($V(0) = \sum_{\nu=-N}^N c_\nu(0) = 1$) was distributed symmetrically about the origin so that $c_\nu(0) = 1/11$ for $-5 \leq \nu \leq 5$ and $c_\nu(0) = 0$ otherwise. A wider initial distribution would require N to be larger, and one narrower seems unrealistic to us; in any case, this choice of initial conditions is convenient, but not necessary, to obtain the conclusions described in the following sections. We chose $\gamma =$

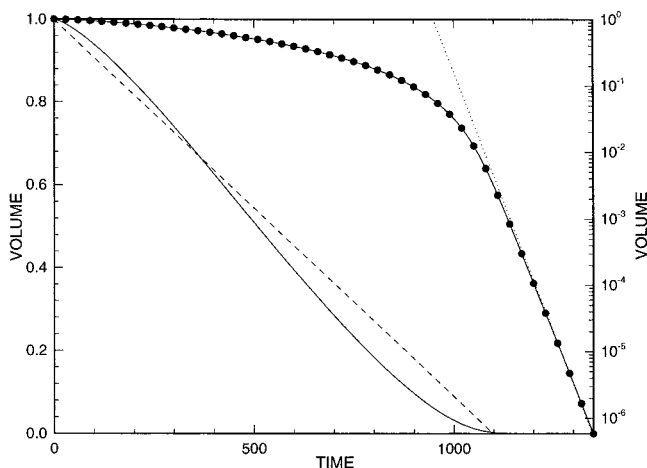


Figure 1. Depletion of the mass vs time for the periodic array of traps for P. The solid curve and solid circles correspond to the linear and logarithmic axes, respectively. The dashed and dotted curves show the roughly linear and exponential behavior, respectively.

0.0001 and $c^+ = 2\gamma$, independently of ν ; thus $\gamma\lambda^2 \ll D$ for P. We then solved (3) with a second-order (in time) Runge–Kutta algorithm¹⁸ for a fixed time step of $\Delta\tau = 0.1$; one trajectory for each configuration of traps, until $\max_{\nu}\{c_{\nu}(\tau_{\text{stop}})\} = 10^{-8}$ (which defines τ_{stop}).

Our choice of $\gamma = 10^{-4}$ corresponds to a moderately efficient biological degradation rate of trichloroethene in the laboratory, when reasonable choices are made for the unit length, unit time, and trap size. For the sake of discussion and without affecting any of our results (which are independent of specific values for these parameters), we show how reasonable choices for these parameters might be made. One may assume that there is on average one trap per cubic centimeter of matrix. This choice would give $\lambda = 1$ cm, and with $n = 10$ above, the unit length would become 0.1 cm. With this choice and $D = 10^{-5}$ cm²/s (unity in our reduced units), which is typical for the diffusion of molecules in water, one would obtain the unit time of 1000 s. Next, each trap, in a moderately fertile matrix, would consist of 10^{-5} g of active cells, recalling that the cells have a density of 10^{12} cells/g and that a fertile soil is thought to have more than 10^7 active cells/cm³ of matrix.⁵ Finally, one may assume that the density of the substrate is near that of water. Combining all of these considerations implies that our choice of $\gamma = 10^{-4}$ would correspond to about 1 $\frac{\text{g}_{\text{substrate}}}{\text{g}_{\text{cell}}}$ day). In optimized bioreactors, with extra nutrients injected, the biodegradation rate for trichloroethene can reach 100 $\frac{\text{g}_{\text{substrate}}}{\text{g}_{\text{cell}}}$ day),¹⁹ but such a high degradation rate would not be achieved in soils without extra nutrients, stirring, and temperature control, so we chose to be conservative.

III. Results

We calculated one trajectory for P. For R, we calculated one trajectory for each of 100 independent randomly generated trap configurations on the lattice, collecting values from each trajectory every 100 time steps. We found the crossover time τ^* numerically by maximizing

$$\dot{V} \approx V(\tau + \Delta\tau) + V(\tau - \Delta\tau) - 2V(\tau) \quad (4)$$

with respect to τ . We show first the total substrate mass (or volume) $V(\tau)$, defined by $V(\tau) \equiv \sum_{\nu} c_{\nu}(\tau)$. The solutions for P are qualitatively indistinguishable from those provided by eq 3 where ρ is constant everywhere on the line. Figure 1 shows that for P, V follows the anticipated pattern of substantially linear

TABLE 1: Values of Parameters for Homogeneous, Ordered, and Disordered Configurations of Traps^a

parameters	no diffusion, one trap (eq 1)	periodic traps (case P)	random traps (case R)
t^*	990	1050	930
$c_{\text{max}}(t^*)$	0.00010	0.00030	0.0026
$V(t^*)$	0.00010	0.012	0.14
t_{stop}	1040	1350	3000
$V(t_{\text{stop}})$	10^{-8} (exact)	5.9×10^{-7}	3.1×10^{-7}

^a For R, the values are the means obtained by averaging over the 100 trap configurations and are reported to only two significant figures.

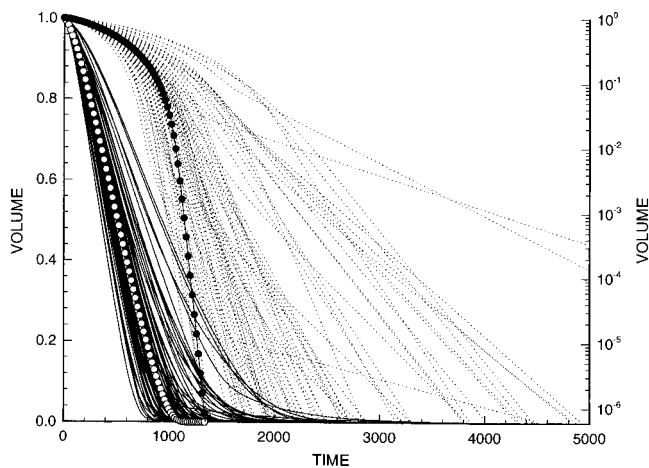


Figure 2. Depletion of the mass vs time for R. The solid and dotted curves correspond to the linear and logarithmic axes, respectively. Results from Figure 1 (P) are superimposed for reference: white and black circles correspond to the linear and logarithmic axes, respectively.

decay until the crossover time τ^* is reached, after which it undergoes essentially exponential decay, indicated by the linear behavior in the logarithmic plot. The results are summarized in Table 1. Even with substantial diffusion, the behavior of V in P is not substantially different from the behavior expected of a system with no net transport (eq 1), e.g., a reaction in a continuously stirred flask. The crossover and stopping times (τ^* and τ_{stop} , respectively) for the “single-site” nondiffusing system are close to the values obtained for P. In other words, P is reaction-limited, not diffusion-limited.

The degradation of the substrate in the presence of randomly placed traps (R) is more difficult to assess. We did not detect in R the “stretched exponential” decay ($c(t) \propto \exp(-t^\beta)$, $0 < \beta < 1$) that is often associated with dispersive kinetics⁹ before our self-imposed concentration limit was achieved. Instead, we found that at least 12 decades of concentration reduction are required in this model before we observe the beginning of stretched exponential decay. Without further work, we might have concluded that no significant anomalies would occur, because the degradation remains reaction-limited in this case also, for all times and concentrations of interest. Nevertheless, the trajectories in R display an abundance of anomalous and widely varying kinetic behavior. Figure 2 shows $V(\tau)$ for each of the trajectories in R and, for comparison, the trajectory calculated for P: The broad distribution of V is evident. Similar considerations apply qualitatively to the maximum concentration c_{max} . The lack of sensitivity to the initial concentration distribution can be inferred from the fact that the anomalies became apparent at times that are greater than the time required for the initial concentration to spread several times larger than the initial width. Consequently, little if any of the variation in the trajectories is due to fluctuations in the placement of traps near

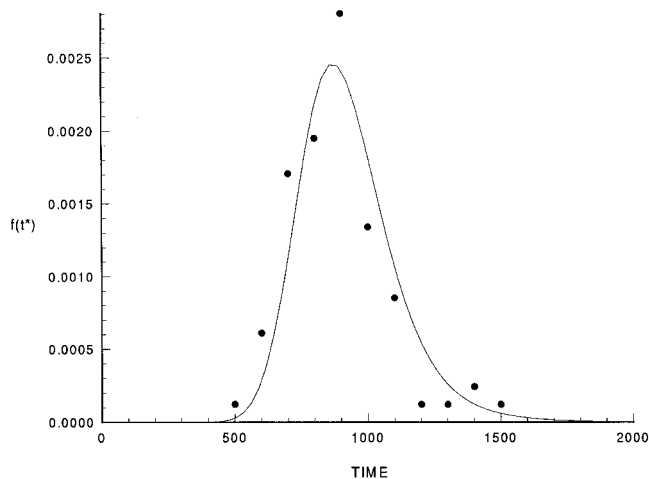


Figure 3. Distribution of crossover times from case R. The solid curve corresponds to the 4-moment maximum-entropy distribution; solid circles show the results of binning.

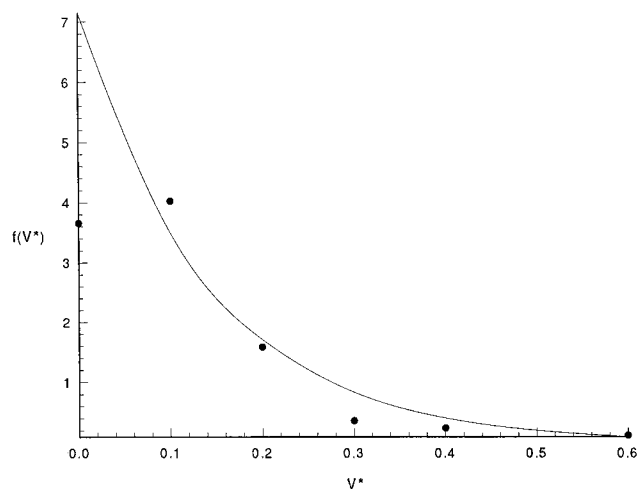


Figure 4. Distribution of mass at the crossover time from case R. Symbols are as in Figure 3.

the initial concentration distribution, but instead it is due to the much wider variation in the placement of traps further away from the initial distribution.

For each configuration we computed the crossover time τ^* and $V^* = V(\tau^*)$ via (4). The distributions of both τ^* and V^* , which were reconstructed from their moments via maximum entropy,²⁰ are shown in Figures 3 and 4, respectively. The distribution of τ^* is narrow and nearly normally distributed, so that the configuration average of τ^* is also nearly a typical τ^* . Furthermore, the configuration average of τ^* for R is nearly that of P. In contrast, the distribution of the V^* is very broad; in fact, it is nearly exponentially distributed. Thus the configuration average of V^* is very far from the typical V^* . Figure 5 shows that the distribution of stopping times τ_{stop} is complicated. The bulge in its tail persists far beyond the configuration average and gives it a bimodal character. Furthermore, the mean τ_{stop} is both longer than the typical τ_{stop} (corresponding to the maximum of the distribution) and more than twice as long as the mean for P (Table 1). Figure 6 shows the distribution of $V(\tau_{\text{stop}})$, which is broad, possesses a long tail, and is also apparently bimodal. These results together show that a wide range of kinetic behavior, including an anomalous increase in the time required to finish degradation, can result from nothing more than disorder in the placement of degrading sites in the subsurface.

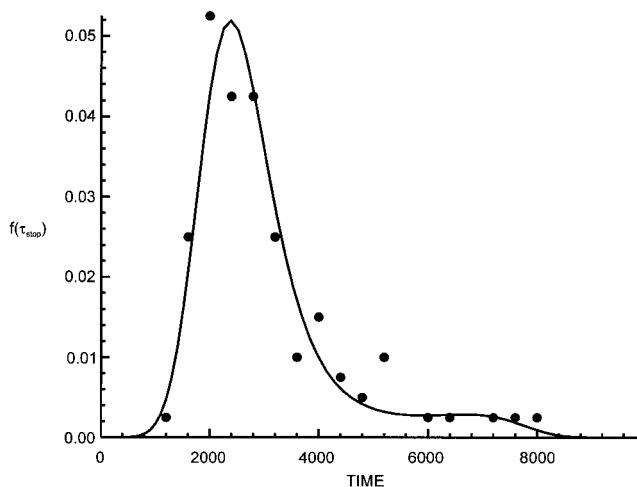


Figure 5. Distribution of stopping times from case R. Symbols are as in Figure 3.

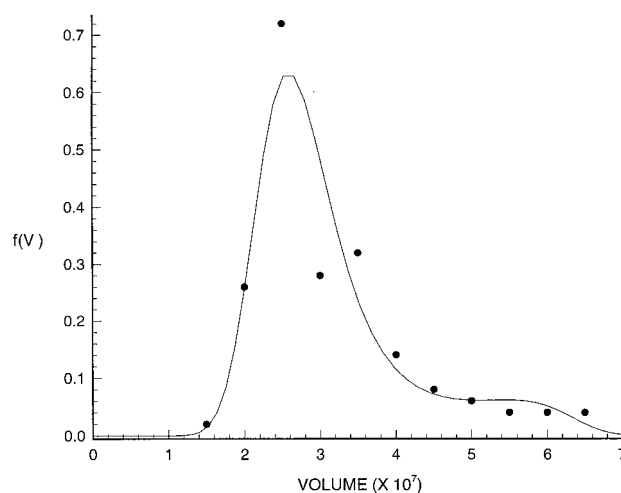


Figure 6. Distribution of mass at the stopping time from case R. Symbols are as in Figure 3.

IV. Discussion and Conclusions

We began by asking why the degradation kinetics that are measured in a homogeneous system in the laboratory, e.g., a continuously stirred flask, often seem faster, and much more narrowly distributed, than the degradation kinetics in the field. The complexity of the subsurface matrix, toxicity responses, trophic interactions, and threshold effects, among many others, all surely play a role in the outcome.²¹ We have shown that this outcome also can be obtained simply from changing the placement of fixed microorganisms from ordered (periodic) to disordered (random) in an otherwise homogeneous subsurface matrix. Specifically, we found that the spatial fluctuations created by a random distribution of identical traps can substantially increase the mean time for biodegradation to reduce the initial concentration of contaminant substrate to prescribed levels. More importantly, the breadth and bimodality of the distributions of the stopping times imply that any one configuration of traps can support substantially different degradation behavior from any other, even though both configurations were generated from the same distribution.

To apply the mean degradation behavior obtained in the laboratory directly to the situation in the field, where there is no opportunity to sample other configurations, the degradation rate for any particular configuration would need to have only a small deviation from the average. Our results suggest that,

instead, the dispersion in degradation behavior introduced by the disorder in the trap placement is a factor that should be recognized explicitly in the assessment of intrinsic biodegradation restoration schemes. The kind of calculations employed here, for an ensemble of configurations rather than for a single spatially averaged configuration, can provide reasonable bounds on the range of expected behavior of the contaminant substrate for a more realistic assessment of intrinsic biodegradation schemes for the restoration of contaminated soils.

Acknowledgment. R.A.L. thanks the Maui High Performance Computing Center for computer time under USAF Philips Laboratory Cooperative Agreement F29601-93-2-0001. R.A.L. and D.L.S. thank L. Pratt (Los Alamos) and INEEL colleagues G. Bala, J. Barnes, R. Berry, R. Cherry, P. Gostomski, M. Hamilton, R. Lehman, G. Redden, and R. Starr for helpful discussions. R.A.L. and D.L.S. were supported by DOE under Contract DE-AC07-94ID13223. T.R.G. was supported by DOE through the Environmental Management Science Program.

References and Notes

- (1) National Research Council. *In Situ Bioremediation: When Does It Work?* National Academy Press: Washington, DC, 1993.
- (2) Wilson, J. T.; McNabb, J. F.; Balkwill, D. L.; Ghiorse, W. C. *Groundwater* **1983**, *21*, 134–142.
- (3) Balkwill, D. L.; Ghiorse, W. C. *Appl. Environ. Microbiol.* **1985**, *50*, 580–588.
- (4) Stoner, D. L. In *Biotechnology for the Treatment of Hazardous Waste*; Stoner, D. L., Ed.; Lewis Publishers: Boca Raton, FL, 1994.
- (5) Alexander, M. *Biodegradation and Bioremediation*; Academic Press: San Diego, CA, 1994.
- (6) Baker, K. H.; Berson, D. S. *Bioremediation*; McGraw-Hill: New York, NY, 1994.
- (7) Madsen, E. L. *Environ. Sci. Technol.* **1991**, *25*, 1662–1673.
- (8) Dunlap, D. H.; LaViolette, R. A.; Parris, P. E. *J. Chem. Phys.* **1994**, *100*, 8293–8300.
- (9) Plonka, A. *Annu. Rep. Prog. Chem., Sect. C* **1994**, *91*, 107–174.
- (10) Brockman, F. J.; Murray, C. J. *FEMS Microbiol. Rev.* **1997**, *20*, 231–247.
- (11) Madigan, M. T.; Martinko, J. M.; Parker, J. *Brock Biology of Microorganisms*, 8th ed.; Prentice Hall: Englewood Cliffs, NJ, 1997; Chapter 14.
- (12) Matheron, G.; de Marsily, G. *Water Resour. Res.* **1980**, *16*, 901–917.
- (13) Bear, J. *Dynamics of Fluids in Porous Media*; Dover Publishers: New York, NY, 1988; Chapter 10.
- (14) Domenico, P. A.; Schwartz, F. W. *Physical and Chemical Hydrogeology*; John Wiley: New York, NY, 1990; Chapter 10.
- (15) Shishido, M.; Toda, M. *Biotechnol. Bioeng.* **1996**, *50*, 709–717.
- (16) Howard, P. H.; Boethling, R. S.; Jarvis, W. F.; Meylan, W. M.; Michalenko, E. M. *Handbook of Environmental Degradation Rates*; Lewis Publishers: Boca Raton, FL, 1991.
- (17) Norris, R. D. In *Handbook of Bioremediation*; Matthews, J. E., Ed.; Lewis Publishers: Boca Raton, FL, 1994.
- (18) Lambert, J. D. *Computational Methods in Ordinary Differential Equations*; John Wiley: New York, NY, 1973.
- (19) Jain, M. K.; Criddle, C. S. In *Biotransformations: Microbial Degradation of Health Risk Compounds*; Singh, V. P., Ed.; Elsevier Science BV: Amsterdam, The Netherlands, 1995. The rates reviewed there are zeroth-order rates. However, some others report first-order degradation rates, e.g., refs 22 and 23. If the degradation rate is of hyperbolic form as in our eq 3, then both zeroth- and first-order rates might be observed, depending upon the substrate concentration.
- (20) Agmon, N.; Alhassid, Y.; Levine, R. D. *J. Comput. Phys.* **1979**, *30*, 250–258.
- (21) Adriaens, P.; Hickey, W. J. In *Biotechnology for the Treatment of Hazardous Waste*; Stoner, D. L., Ed.; Lewis Publishers: Boca Raton, FL, 1994.
- (22) Arvin, E. *Water Resour. Res.* **1991**, *25*, 873–881.
- (23) Strandberg, G. W.; Donaldson, T. L.; Farr, L. L. *Environ. Sci. Technol.* **1989**, *23*, 1422–1425.